IEEE Photonics Journal
An IEEE Photonics Society Publication

Open Access

Ultra-Broadband Silicon-Wire Polarization Beam Combiner/Splitter Based on a Wavelength Insensitive Coupler With a Point-Symmetrical Configuration

Volume 6, Number 1, February 2014

Takui Uematsu
Tetsuya Kitayama
Yuhei Ishizaka, Student Member, IEEE
Kunimasa Saitoh, Member, IEEE

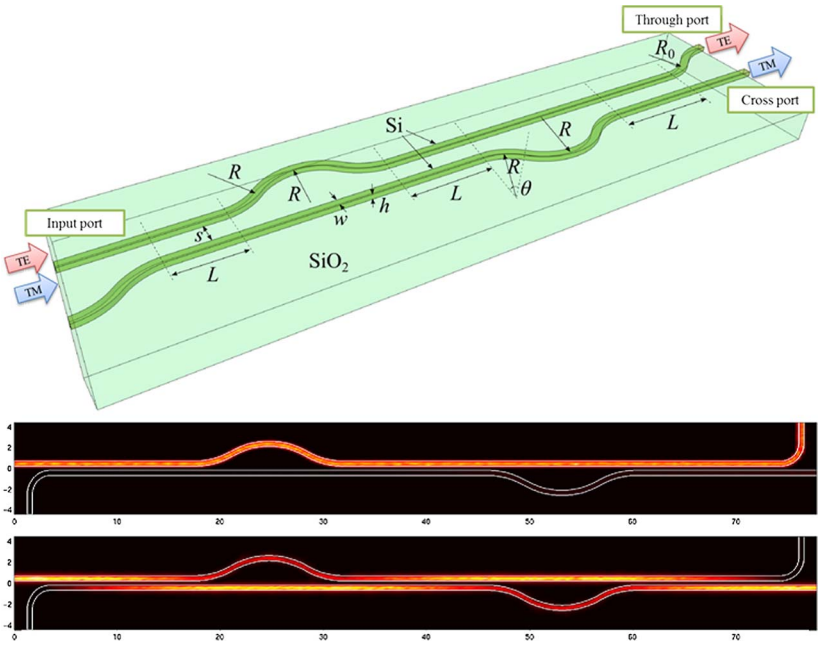

DOI: 10.1109/JPHOT.2014.2302808
1943-0655 © 2014 IEEE

Ultra-Broadband Silicon-Wire Polarization Beam Combiner/Splitter Based on a Wavelength Insensitive Coupler With a Point-Symmetrical Configuration

Takui Uematsu, Tetsuya Kitayama, Yuhei Ishizaka, *Student Member, IEEE*, and Kunimasa Saitoh, *Member, IEEE*

Graduate School of Information Science and Technology, Hokkaido University, Sapporo 060-0808, Japan

DOI: 10.1109/JPHOT.2014.2302808

Manuscript received December 16, 2013; revised January 11, 2014; accepted January 16, 2014. Date of publication January 27, 2014; date of current version February 4, 2014. Corresponding author: T. Uematsu (e-mail: uematsu@icp.ist.hokudai.ac.jp).

Abstract: An ultrabroadband silicon wire polarization beam combiner/splitter (PBCS) based on a wavelength-insensitive coupler is proposed. The proposed PBCS consists of three identical directional couplers and two identical delay lines. We design the PBCS using the 3-D finite element method. Numerical simulations show that the proposed PBCS can achieve the transmittance of more than 90% over a wide wavelength range from 1450 to 1650 nm for both TE and TM polarized modes.

Index Terms: Silicon nanophotonics, waveguide devices, finite element methods.

1. Introduction

Silicon-wire waveguides have attracted attention for ultra-small optical circuits. So far, various kinds of silicon wire devices such as ring resonators [1], arrayed waveguide gratings [2], multi-mode interference (MMI) coupler [3], mode multiplexer [4] have been proposed. However, silicon-wire waveguides have large polarization dependence due to the high refractive index contrast. To overcome this problem, the polarization diversity system which includes a polarization beam combiner (PBC) and a polarization beam splitter (PBS) has been presented [5]. In the polarization diversity system, a PBS splits TE and TM modes at first, and a PBC combines the TE and TM modes at last. Therefore, a PBC and a PBS with high performance are desired.

Various types of silicon-wire PBCs/PBSs (PBCSs) have been proposed based on a symmetrical directional coupler (DC) [6], asymmetrical DCs [7]–[9], a bent DC [10], [11], MMI couplers [12], [13], Mach–Zehnder interferometers (MZIs) [14], and plasmonic waveguides [15]–[17]. Though DC-based PBSs have the advantage of small footprints, simplicity, and easy fabrication, DC-based PBSs are sensitive to wavelength change. More investigations for expanding the bandwidth of the DC-based PBSs are needed to achieve the broadband polarization diversity system.

In this paper, we propose a PBCS based on a wavelength-insensitive-coupler (WINC) [18] to realize an ultra-broadband PBCS. The WINC-based PBCS consists of three identical directional couplers and two identical delay lines with a point-symmetrical configuration. We design the WINC-based PBCS using the 3-D finite element method [19]. Numerical simulations show that the proposed

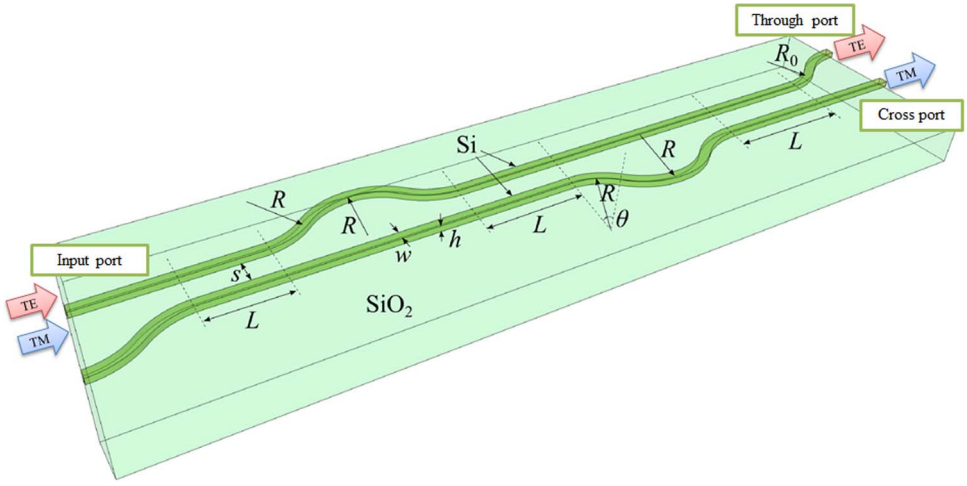

Fig. 1. Structure of the WINC-based PBCS. The PBCS is based on silicon wire waveguide. The materials of the substrate and upper-cladding are silica and air, respectively.

PBCS can achieve the transmittance of more than 90% over a wide wavelength range from 1450 nm to 1650 nm for both TE and TM polarized modes. We also calculate the fabrication tolerance. The proposed PBCS has relatively good tolerance to fabrication errors.

2. Design and Characteristics of WINC-Based PBS

Fig. 1 shows the structure of the proposed PBCS. The proposed PBCS is based on the silicon wire PBS with the symmetrical DC [6] and the WINC with a point-symmetrical configuration [18]. In a symmetrical DC based on silicon wire, the coupling length for the TM mode is much shorter than that for TE mode due to large difference between propagation constants of TE mode and TM mode [6]. Thus, a symmetrical DC works as a PBCS. However, the DC-based PBCS is strongly dependent on wavelength change.

We then use the WINC to attain a broadband PBCS. The WINC with a MZI configuration has been proposed to make a coupler independent on wavelength change [20]. The wavelength-flattened coupling characteristics are realized by using the WINC. However, it is difficult to flatten the high-transmittance bands of a cross port output [18]. Then, the WINC with a point-symmetrical configuration has been presented [18]. The WINC with a point-symmetrical configuration achieves the high-transmittance of a cross port output over a wide wavelength range [18]. We then utilize the WINC with a point-symmetrical configuration for the proposed PBCS in order to obtain an ultra-broadband PBCS.

In this paper, we assume a silicon-on-insulator (SOI) wafer with a silicon thickness of $h = 240$ nm and the refractive indices of Si, SiO_2, and air are 3.447, 1.444, and 1.00, respectively. The waveguide width w and the gap between the waveguides s are respectively chosen to $w = 500$ nm and $s = 400$ nm for TE mode not to be coupled in the coupling regions. The gap is large enough to make the fabrication easy. The bending radius R_0 at the end of the PBCS to make the two waveguides separated is set to $R_0 = 2$ μm to realize a TE-through polarizer which filters out the undesired TM mode at the through port.

In order to obtain an ultra-broadband PBCS, we need to design the length of the coupling regions and the path length difference by the two delay lines appropriately. In this paper, the path length difference by the delay line is adjusted by changing the bending radius R of the delay line, while the arc-angle is fixed to $\theta = \pi/6$, as shown in Fig. 2. Fig. 3 shows the design concept of the WINC-based PBCS. The WINC-based PBCS is composed of two identical WINC-based 3-dB couplers cascaded to be a point-symmetrical configuration. The WINC-based 3-dB coupler is designed for TM mode to be coupled 50% over a wide wavelength range according to design rules proposed in

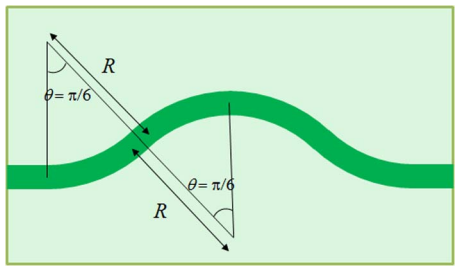

Fig. 2. Structure of the delay line. The arc-angle is fixed to $\theta = \pi/6$. The path length difference is controlled by changing R.

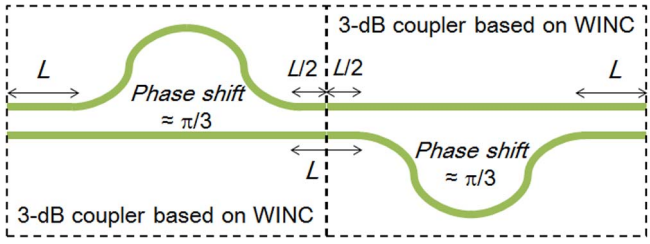

Fig. 3. Design concept of the WINC-based PBCS. The proposed PBCS is composed of two identical WINC-based 3-dB couplers cascaded to be a point-symmetrical configuration. The 3-dB coupler based on the WINC is designed for TM mode to be coupled 50% over a wide wavelength range according to design rules proposed in Ref. [21]. The lengths L and $L/2$ in the WINC-based 3-dB coupler Fig. 3 should be full-coupling length and half-coupling length for TM mode, respectively, and the phase shift by the delay line should be around $\pi/3$.

Ref. [21]. From Ref. [21], the length L and $L/2$ in the WINC-based 3-dB coupler shown in Fig. 3 should be full-coupling length and half-coupling length for TM mode, respectively, and the phase shift by the delay line should be around $\pi/3$.

Thus, from Fig. 3, the length L of the coupling region of the WINC-based PBS should be chosen for most of the TM mode to be coupled to the other waveguide in each coupling region, and the bending radius R of the delay lines should be chosen for phase difference between the waveguides by the delay line to be around $\pi/3$, because two identical 3-dB couplers based on the WINC are cascaded to be a point-symmetrical configuration, as shown in Fig. 3. In this paper, we set to $L = 14.0$ μm and $R = 7.2$ μm to make the transmittance for the case of inputting TM mode as high as possible over a wide wavelength range.

Fig. 4 shows the wavelength dependence of the normalized output powers at the cross port and the through port when (a) TM mode and (b) TE mode are input, respectively. The solid lines and dashed lines in Fig. 4(a) represent the results of the WINC-based PBCS and DC-based PBCS, respectively. From Fig. 4(a), the normalized output power at the cross port of the WINC-based PBCS is more than 0.9 over a wide wavelength range from 1450 nm to 1650 nm, while the DC-based PBCS is more sensitive to wavelength change. The proposed structure can expand the bandwidth with high efficiency. In addition, from Fig. 4(b), the normalized output power at the through port is more than 0.93 over a wide wavelength range from 1450 nm to 1650 nm, and is not sensitive to wavelength change because the TE coupling is smaller due to the longer coupling distance of the TE mode which is a result of more confinement of the TE mode to the core region compared to the TM mode. The coupling length for TE mode at wavelengths of 1450 nm, 1550 nm, and 1650 nm are respectively 1089 μm, 500 μm, 240 μm, which is much longer than that for TM mode (around 14 μm). It is possible to expect that the normalized output powers of TE and TM modes at the input port are more than 0.9 over a wide wavelength range from 1450 nm to 1650 nm when TE mode is input into the through port and TM mode is input into the cross port, because the

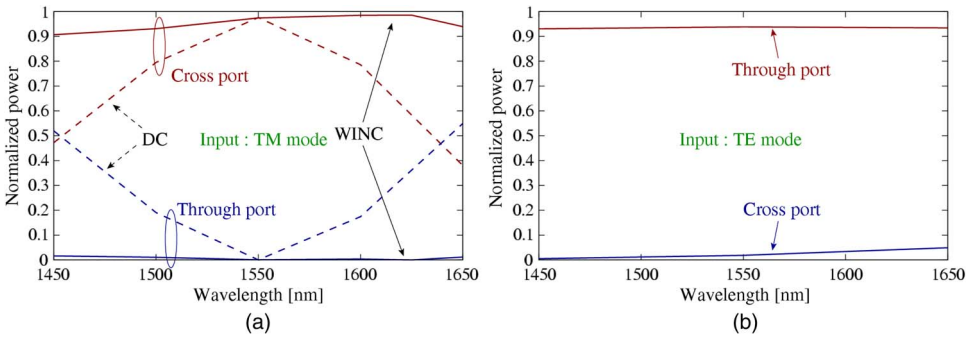

Fig. 4. Wavelength dependence of the designed PBCS when (a) TM mode and (b) TE mode are input, respectively. The solid lines and dashed lines represent results of the WINC-based and DC-based PBCS, respectively.

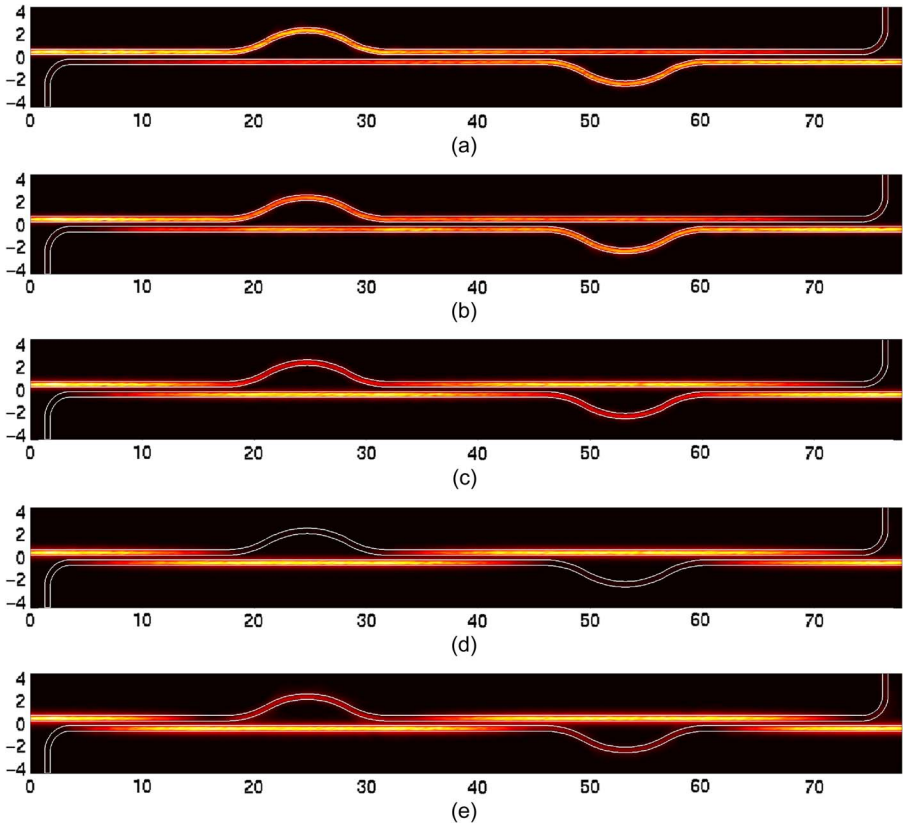

Fig. 5. Field distributions of the designed PBCS when TM mode is input at wavelengths of (a) 1450 nm, (b) 1500 nm, (c) 1550 nm, (d) 1600 nm, and (e) 1650 nm.

WINC-based PBCS has the optical reciprocity. Thus, the proposed PBCS is one of the promising PBCs for the broadband polarization diversity system.

Fig. 5 shows the field distributions of the proposed PBCS when TM mode is input at wavelengths of (a) 1450 nm, (b) 1500 nm, (c) 1550 nm, (d) 1600 nm, and (e) 1650 nm. We can see that most of the input TM mode is coupled and output at the cross port at each wavelength, though the field distributions are different from each other. Fig. 6 shows the field distributions of the proposed PBCS when TE mode is input at wavelengths of (a) 1450 nm, (b) 1550 nm, and (c) 1650 nm. We can confirm that the TE mode is output at the through port without almost any coupling.

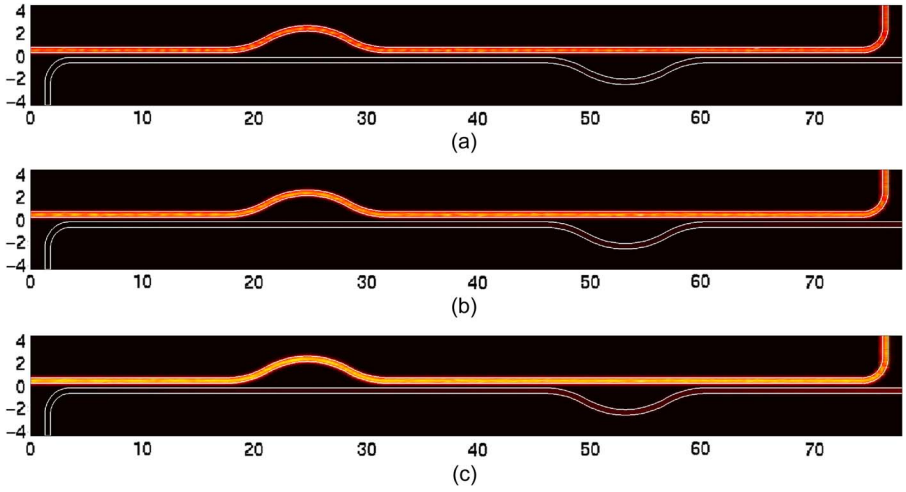

Fig. 6. Field distributions of the designed PBCS when TE mode is input at wavelengths of (a) 1450 nm, (b) 1550 nm, and (c) 1650 nm.

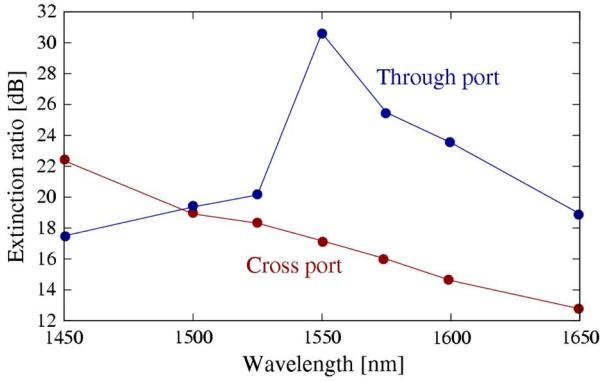

Fig. 7. Wavelength dependence of extinction ratio of the WINC-based PBS.

Fig. 7 shows the wavelength dependence of the extinction ratio at the through port and cross port. The extinction ratio at the through port and cross port are defined as follows:

$$(\text{extinction ratio at the through port}) = 10\log_{10}\frac{P_{TE,through}}{P_{TM,through}} \quad (1)$$

$$(\text{extinction ratio at the cross port}) = 10\log 10\frac{P_{TM,cross}}{P_{TE,cross}} \quad (2)$$

where $P_{TE,through}$ and $P_{TE,cross}$ respectively represent the normalized output power at the through port and cross port when TE mode is input. Similarly, $P_{TM,through}$ and $P_{TM,cross}$ respectively represent the normalized output power at the through port and cross port when TM mode is input. From Fig. 7, the extinction ratio at the through port and the cross port are respectively more than 17 dB and 13 dB over a wavelength range from 1450 nm to 1650 nm. The extinction ratio at the cross port can be improved by making the gap s larger or making the waveguide width w wider to suppress the coupling of TE mode in the coupling regions. Moreover, it can be expected that the extinction ratio can be improved by cascading several WINC-based PBCSs at the end of the WINC-based PBCS as demonstrated in Refs. [6], [22], and using another DC-based PBS such as [7]–[10] instead of the symmetrical DC-based PBS in the coupling regions.

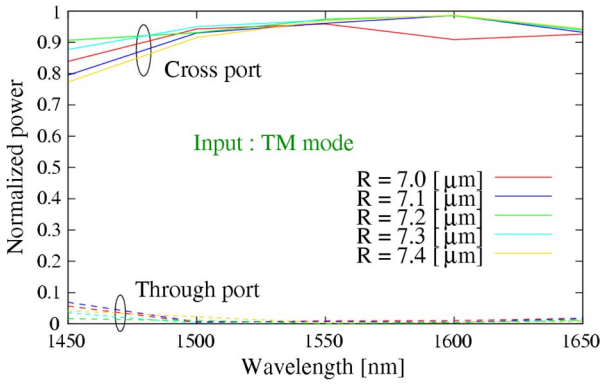

Fig. 8. *R* dependence of the WINC-based PBCS as a function of wavelength when TM mode is input. The solid lines and dashed lines represent results at the cross port and through port, respectively.

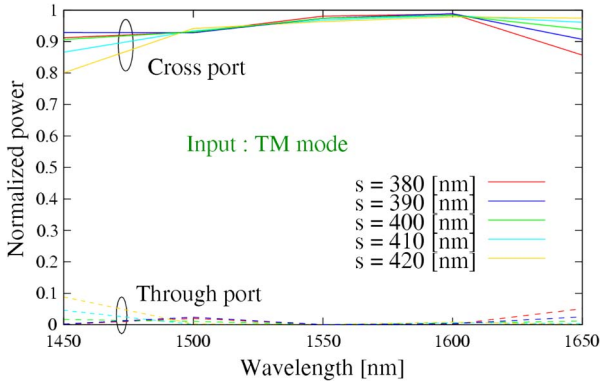

Fig. 9. *s* dependence of the WINC-based PBCS as a function of wavelength when TM mode is input. The solid lines and dashed lines represent results at the cross port and through port, respectively.

Finally, we calculate the fabrication tolerance of the WINC-based PBCS. We calculate the fabrication tolerance for only TM mode because the normalized output power for TE mode is still insensitive to wavelength change, as shown in Fig. 4(b), due to almost no coupling for TE mode. Figs. 8 and 9 show the wavelength dependence of the normalized output power when the bending radius *R* of the delay lines and the gap *s* changes for the case of inputting TM mode, respectively. From Fig. 8, when the *R*variation is as large as ± 0.2 μm, the normalized output power at the cross port is over 0.77 over a wide wavelength range from 1450 nm to 1650 nm. Moreover, from Fig. 9, even when the gap variation is as large as ± 0.2 μm, the normalized output power at the cross port is over 0.8 over a wide wavelength range from 1450 nm to 1650 nm. Fig. 10(a) and (b) shows the normalized output powers when there is a waveguide (a) width *w* or (b) height *h* variation for the case of inputting TM mode at a wavelength of 1550 nm. When the *w* variation is as large as ± 50 nm, the normalized output power at the cross port is more than 0.94, as shown in Fig. 10(a). In addition, when the *h* variation is as large as ± 20 nm, the normalized output power at the cross port is more than 0.88, as shown in Fig. 10(b). Thus, the WINC-based PBCS has a relatively large fabrication tolerance.

3. Conclusion

We have proposed an ultra-broadband PBCS based on a WINC with a point-symmetrical configuration. The proposed PBCS consists of three identical directional couplers and two identical

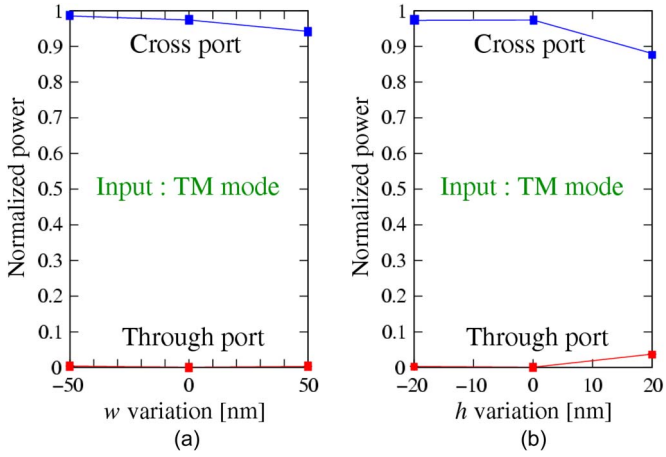

Fig. 10. Normalized output powers when there is a waveguide (a) width w or (b) height h variation for the case of inputting TM mode at a wavelength of 1550 nm. Blue and red lines show the output powers at the cross port and through port, respectively.

delay lines with a point-symmetrical configuration. We have designed the proposed PBCS using the 3-D finite element method. Numerical simulations showed that the proposed PBCS can achieve the transmittance of more than 90% over a wide wavelength range from 1450 nm to 1650 nm for both TE and TM polarized modes. Thus, the proposed PBCS is one of the promising PBCs for the broadband polarization diversity system. We have also calculated the extinction ratio and the fabrication tolerance. The proposed PBCS has good tolerance to fabrication errors. The extinction ratio at the through port and cross port are respectively more than 17 dB and 13 dB over a wavelength range from 1450 nm to 1650 nm. The extinction ratio can be improved by cascading several WINC-based PBCSs at the end of the WINC-based PBCS, and using another DC-based PBS with higher extinction ratio compared with the symmetrical DC-based PBS in the coupling regions.

References

[1] B. E. Little, J. S. Foresi, E. R. Thoen, S. T. Chu, H. A. Haus, E. P. Ippen, L. C. Kimerling, and W. Greene, "Ultra-compact $Si-SiO_2$ microring resonator optical channel dropping filters," *IEEE Photon. Technol. Lett.*, vol. 10, no. 4, pp. 549–551, Apr. 1998.
[2] K. Sasaki, F. Ohno, A. Motegi, and T. Baba, "Arrayed waveguide grating of 70×60 μm^2 size based on Si photonic wire waveguides," *Electron. Lett.*, vol. 41, no. 14, pp. 801–802, Jul. 2005.
[3] Z. Sheng, Z. Wang, C. Qiu, L. Li, A. Pang, A. Wu, X. Wang, S. Zou, and F. Gan, "A compact and low-loss MMI coupler fabricated with CMOS technology," *IEEE Photon. J.*, vol. 4, no. 6, pp. 2272–2277, Dec. 2012.
[4] T. Uematsu, Y. Ishizaka, Y. Kawaguchi, K. Saitoh, and M. Koshiba, "Design of a compact two-mode multi/demultiplexer consisting of multimode interference waveguides and a wavelength-insensitive phase shifter for mode-division multiplexing transmission," *J. Lightw. Technol.*, vol. 30, no. 15, pp. 2421–2426, Aug. 2012.
[5] T. Barwicz, M. R. Watts, M. A. Popovic, P. T. Rakich, L. Socci, F. X. Kartner, E. P. Ippen, and H. I. Smith, "Polarization-transparent microphotonic devices in the strong confinement limit," *Nature Photon.*, vol. 1, no. 1, pp. 57–60, Jan. 2007.
[6] H. Fukuda, K. Yamada, T. Tsuchizawa, T. Watanabe, H. Shinojima, and S. Itabashi, "Ultrasmall polarization splitter based on silicon wire waveguides," *Opt. Exp.*, vol. 14, no. 25, pp. 12401–12408, Dec. 2006.
[7] M. Komatsu, K. Saitoh, and M. Koshiba, "Design of miniaturized silicon wire and slot waveguide polarization splitter based on a resonant tunneling," *Opt. Exp.*, vol. 17, no. 21, pp. 19225–19233, Oct. 2009.
[8] D. Dai, Z. Wang, and J. E. Bowers, "Ultrashort broadband polarization beam splitter based on an asymmetrical directional coupler," *Opt. Lett.*, vol. 36, no. 13, pp. 2590–2592, Jul. 2011.
[9] D. Dai, "Silicon polarization beam splitter based on an asymmetrical evanescent coupling system with three optical waveguides," *J. Lightw. Technol.*, vol. 30, no. 20, pp. 3281–3287, Oct. 2012.
[10] D. Dai and J. E. Bowers, "Novel ultra-short and ultra-broadband polarization beam splitter based on a bent directional coupler," *Opt. Exp.*, vol. 19, no. 19, pp. 18614–18620, Sep. 2011.
[11] J. Wang, D. Liang, Y. Tang, D. Dai, and J. E. Bowers, "Realization of an ultra-short silicon polarization beam splitter with an asymmetrical bent directional coupler," *Opt. Lett.*, vol. 38, no. 1, pp. 4–6, Jan. 2013.

[12] B. Yang, S. Shin, and D. Zhang, "Ultrashort polarization splitter using two-mode interference in silicon phtonic wires," *IEEE Photon. Technol. Lett.*, vol. 21, no. 7, pp. 432–434, Apr. 2009.
[13] A. Hosseini, S. Rahimi, X. Xu, D. Kwong, J. Convey, and R. T. Chen, "Ultracompact and fabrication-tolerant integrated polarization splitter," *Opt. Lett.*, vol. 36, no. 20, pp. 4047–4049, Oct. 2011.
[14] D. Pérez-Galacho, R. Halir, A. Ortega-Moñux, C. Alonso-Ramos, R. Zhang, P. Runge, K. Janiak, H.-G. Bach, A. G. Steffan, and Í. Molina-Fernández, "Integrated polarization beam splitter with relaxed fabrication tolerances," *Opt. Exp.*, vol. 21, no. 12, pp. 14146–14151, Jun. 2013.
[15] C.-L. Zou, F.-W. Sun, C.-H. Dong, X.-F. Ren, J.-M. Cui, X.-D. Chen, Z.-F. Han, and G.-C. Guo, "Broadband integrated polarization beam splitter with surface plasmon," *Opt. Lett.*, vol. 36, no. 18, pp. 3630–3632, Sep. 2011.
[16] F. Lou, D. Dai, and L. Wosinski, "Ultracompact polarization beam splitter based on a dielectric–hybrid plasmonic–dielectric coupler," *Opt. Lett.*, vol. 37, no. 16, pp. 3372–3374, Aug. 2012.
[17] X. Guan, H. Wu, Y. Shi, L. Wosinski, and D. Dai, "Ultracompact and broadband polarization beam splitter utilizing the evanescent coupling between a hybrid plasmonic waveguide and a silicon nanowire," *Opt. Lett.*, vol. 38, no. 16, pp. 3005–3008, Aug. 2013.
[18] K. Jinguji, N. Takato, Y. Hida, T. Kitoh, and M. Kawachi, "Two-port optical wavelength circuits composed of cascaded Mach–Zehnder interferometers with point-symmetrical configurations," *J. Lightw. Technol.*, vol. 14, no. 10, pp. 2301–2310, Oct. 1996.
[19] Y. Ishizaka, Y. Kawaguchi, K. Saitoh, and M. Koshiba, "Three-dimensional finite-element solutions for crossing slot-waveguides with finite core-height," *J. Lightw. Technol.*, vol. 30, no. 21, pp. 3394–3400, Nov. 2012.
[20] K. Jinguji, N. Takato, A. Sugita, and M. Kawachi, "Mach–Zehnder interferometer type optical waveguide coupler with wavelength-flattened coupling ratio," *Electron. Lett.*, vol. 26, no. 17, pp. 1326–1327, Aug. 1990.
[21] B. E. Little and T. Murphy, "Design rules for maximally flat wavelength-insensitive optical power dividers using Mach–Zehnder structures," *IEEE Photon. Technol. Lett.*, vol. 9, no. 12, pp. 1607–1609, Dec. 1997.
[22] L. Chen, C. R. Doerr, and Y.-K. Chen, "Compact polarization rotator on silicon for polarization-diversified circuits," *Opt. Lett.*, vol. 36, no. 4, pp. 469–471, Feb. 2011.